Proceedings of the 37th IAHR World Congress
August 13 – 18, 2017, Kuala Lumpur, Malaysia

FORMATIVE PARAMETERS FOR STABLE ARMOR DEVELOPMENT

STEPHANE BERTIN[1] & HEIDE FRIEDRICH[2]

[1,2] Department of Civil and Environmental Engineering, University of Auckland, Auckland, New Zealand
s.bertin@ymail.com; h.friedrich@auckland.ac.nz

ABSTRACT

Stable fluvial armors, shaped by surface coarsening during selective sediment transport, received considerable attention over the years. Stable armoring is important in river engineering studies. For example, a classical problem is the riverbed degradation downstream of a dam. Our knowledge of whether stable armors can develop with limited sediment supply is still insufficient, yet this is a condition found in many natural gravel-bed rivers. Practically, given a suitable timeframe that allows sediment transport to reduce to approximately zero under a constant flow of water, stable armors can be re-created in laboratory flumes, allowing controlled studies with precise measurements. This study examines the extent to which armor structure is replicable under identical flow and bulk sediment composition. Two sets of experiments were performed using two different bulk sediment mixtures. Unstructured gravel beds were prepared in a laboratory flume and were water-worked successively with two constant discharges until the formation of stable armors. No sediment was fed and selective sediment transport prevailed. Grain-scale digital elevation models (DEMs), as well as bed-surface and bedload compositions, were obtained to quantify the changes due to armoring and to identify the formative parameters. We found bed structure to be more responsive to changes in flow discharge than bed-surface composition, and both armor composition and surface structure were unique given identical formative parameters. This finding is significant as it shows that bed composition alone is not sufficient to describe armor roughness. We discuss the relationships between a fully-developed stable armor and the flow and sediment forming it. The relationships examine the effects of varying the formative parameters onto the armor properties (e.g., composition and roughness), which were extended with the addition of extensive data from previous research.

Keywords: Roughness; remote sensing; photogrammetry; dem; statistical analysis.

1 INTRODUCTION

Stable (also called static) fluvial armors commonly occur in poorly sorted gravel-bed rivers in conditions of partial sediment transport with little to no sediment supply from upstream (Proffitt, 1980; Chin et al., 1994; Gomez, 1994; Vericat et al., 2006). The formation of a stable armor is a stability-seeking mechanism, whereby selective entrainment (winnowing) of fine mobile particles uncovers coarse immobile particles forming a layer typically one grain diameter thick, which isolates the underlying bed material from the flow and prevents further bed degradation (Parker and Klingeman, 1982; Gomez, 1983; Parker and Sutherland, 1990; Richards and Clifford, 1991; Gomez, 1993; Pitlick et al., 2008). Stable armors result from a progressive reduction in sediment transport to practically zero (Gessler, 1967).

In comparison, sediment supply from upstream allows for the progressive equalization between the bedload and the subarmor composition for mobile armors (e.g., Paris, 1992; Marion et al., 2003; Mao et al., 2011). Mobile armors can persist over floods (e.g., Parker and Klingeman, 1982; Wilcock and DeTemple, 2005; Clayton and Pitlick, 2008), as eroded grains are replaced by similar-sized grains originating from upstream, whilst stable armors only persist during floods of a lesser magnitude than the formative flow (e.g., Laronne and Carson, 1976; Proffitt, 1980; Gomez, 1983; Chin et al., 1994; Vericat et al., 2006). In the case of flows above the critical armoring discharge or when uniform sediment prevents selective entrainment, all particle sizes present on the bed are in motion and no armor can form (e.g., Chin et al., 1994). Other protective mechanisms are involved, such as a slope reduction.

Field observations reveal that full mobilization of surface grains in gravel-bed rivers is not a frequent event, with examples indicating full mobilization for floods with a 7-year return period or more (Haschenburger and Wilcock, 2003; Vericat et al., 2006). This suggests a possible wide occurrence of stable armors in nature. In the laboratory, recreating stable armoring allows to study bed-flow interactions and the evolution of a gravel streambed under readily recreated experimental conditions (selective transport and no sediment feed).

Using different flow discharges, past work (e.g., Odgaard, 1984; Chin et al., 1994; Garde et al., 2006) examined the armoring effects onto bed grain-size distribution (GSD). The models developed suggest a specific (i.e. replicable) armor composition, dependent on the parent bed material and the formative discharge. More recently, research on the interactions between flow and sediment has evolved to consider no

only the armor GSD but the actual surface structure and topography (e.g., Lane, 2005; Hodge et al., 2013), since the latter offers new perspectives on bed stability and roughness. Therefore, it is of interest to test the hypothesis that armor topography is replicable given formative parameters.

2 METHODOLOGY

Two sediment mixtures with natural river-worn sands and gravels were used in this study to recreate armored beds in a laboratory flume. For each sediment mixture, three replicated experimental runs were performed, during which an initially screeded flat and poorly-sorted gravel bed was water-worked successively with two discharges until stable armors were formed. Conditions of parallel degradation (i.e. selective entrainment and no sediment feed) prevailed. To assess the reproducibility of our experiments, each run was set up identically and flow conditions were kept as constant as possible within and between runs. In particular, the condition of a constant shear stress despite bed degradation was justified by raising the sediment bed according to the depth of erosion, to maintain bed and water surface slopes steady, a technique used by others before (e.g., Chin et al., 1994; Heays et al., 2014).

2.1. Experimental environment

A non-recirculating tilting flume with glass side-walls, 19 m long, 0.45 m wide and 0.5 m deep, shown in Figure 1A, was used for the experiments. A 1.0 m long, 0.45 m wide and 0.13 m deep sediment recess (called the test section), with a vertically adjustable table that supported the movable sediment bed, was installed 10.4 m from the flume inlet. To facilitate the development of a fully turbulent boundary layer and homogeneous hydraulic conditions, the bed upstream and downstream of the test section was artificially roughened. A sediment trap was installed 0.5 m downstream of the test section and allowed collection of all eroded sediment.

Two coarse sediment mixtures, called sediment 1 and sediment 2 (Figure 1B), were prepared from two distinct, slightly bimodal, alluvial sediments, with size ranging from 0.7 to 35 mm, and used as movable bed materials for the development of stable armors in the sediment recess. Median grain size, D_{50}, was 8.4 mm and 9.2 mm and the sediment geometric sorting was 3.1 and 2.6, for sediment 1 and sediment 2, respectively.

2.2 Experimental procedure

For each run, the well-mixed sediment was placed in the test section, screeded flat to a thickness of 0.13 m, parallel to the flume bed, and leveled with the surrounding fixed beds. The flume slope was held constant at 0.5% throughout the tests.

A short period of low flow was initiated to allow air trapped in the gravel mixture to escape. A constant flow discharge Q_1 = 67 L/s was then applied over 100 hours (see Table I). The flume tail gate was not used, allowing the water depth to naturally adjust, while near uniform flow conditions were attained. After a stable armor had formed, a constant flow rate Q_2 = 84 L/s was applied over 300 hours. For Q_1 and Q_2, the flow was stopped when the sediment transport rate dropped to less than 1% of the initial transport rate measured after two hours at a constant discharge.

2.3 Bed surface measurement and analysis

Measurement of the bed surface, both through air and water, was performed with digital photogrammetry, using a pair of Nikon D5100s (16.4 Mpixel, 23.6 × 15.6 mm^2 sensor size) with Nikkor 20 mm lenses. The cameras were placed 0.3 m apart using a mounting bar and installed 0.65 m vertically above the test section (Figure 1A).

Table I: Flow conditions for the formation of the two successive stable armors. H is flow depth; U is flow depth-averaged velocity; Re = UR_h/v, where R_h is the hydraulic radius and v is the kinematic viscosity of water (taken as 10^{-6} m^2/s); τ_* is Shields stress based on the parent bed D_{50}, calculated as $u^{*2}/(SG-1)gD_{50}$; and Re* = u^*k_s/v is the grain Reynolds number. [1,2]is for the two different sediment mixtures. Low transport rates characterized the study. [I]The shear velocity u* and the equivalent roughness height k_s were estimated from the law-of-the-wall and a velocity profile measured in the centerline of the flume over the fixed roughness bed upstream of the test section, using a Vectrino+ acoustic velocimeter (Nortek®), with 200 Hz sampling rate and 120 s sampling time. 15 measurement points along the lower 75% of the water column were recorded (with 5 points along the lowest 10 mm).

	H (m)	U (m/s)	Re	u* (m/s)	τ_*	Re*	Duration (hrs)
Q_1 = 67 L/s	0.195	0.75	79,300	0.0722[I]	0.044[1] 0.040[2]	513	100
Q_2 = 84 L/s	0.225	0.82	92,800	0.0774[I]	0.050[1] 0.046[2]	526	300

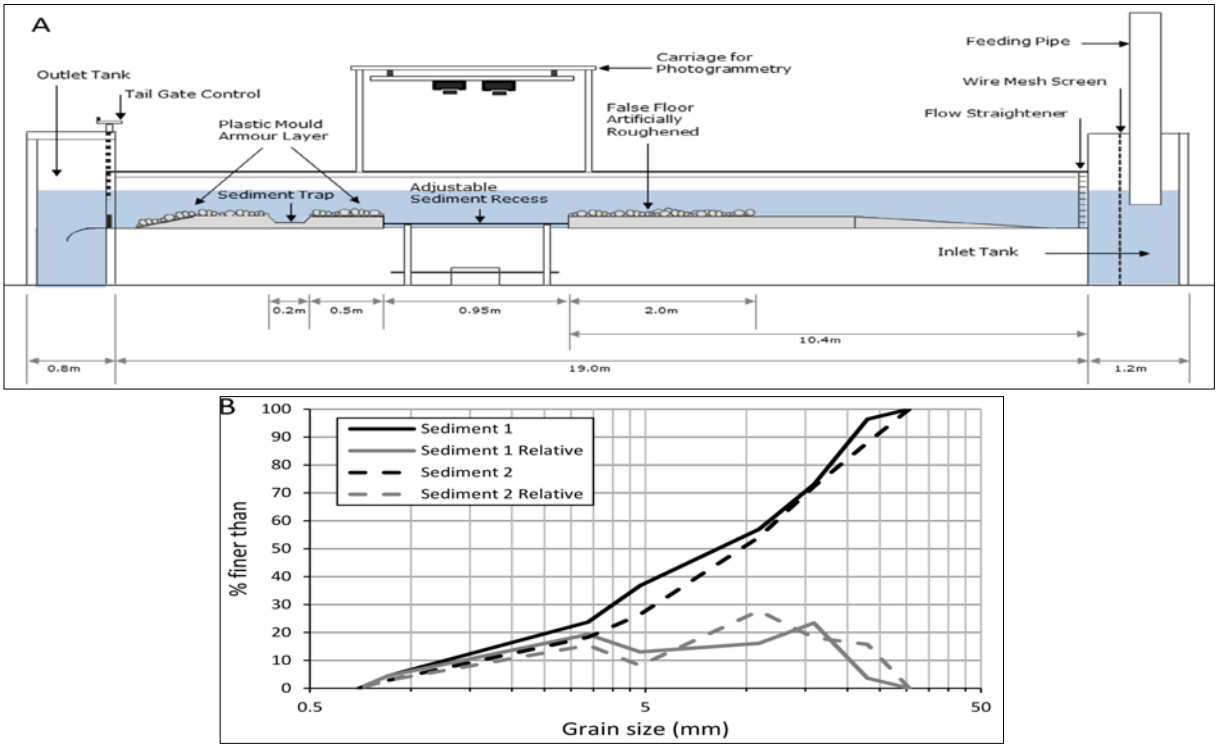

Figure 1. (A) Experimental setup. Flow direction is from right to left. (B) Grain-size distributions (GSDs) of the two sediment mixtures used in the study, obtained after sieving and correcting for the square-hole sieves.

Armor composition and gravel orientation were determined using a single photograph (area: 0.65 × 0.35 m^2, pixel size: 0.15 mm, number of detected sediment grains ~ 1000) and the image-analysis tool Basegrain®. The latter allows for automatic grain separation in digital images of gravel beds and applies Fehr (1987)'s line-sampling method for the results' analysis (Detert and Weitbrecht, 2012). The method was calibrated to minimize differences with a sieve-based grain-size distribution. Grain-size properties of the armors were indexed with "A", to easily distinguish them from properties of the bulk mixtures. For the screeded beds, the composition was assumed equal to the bulk mixtures. Basegrain® also determined the detected grains' a-axis orientation by fitting an ellipse whose areal normalized second-central moment equals that of the grain and computing the angle formed between the ellipse long axis and the flow-orientated image long axis.

To avoid draining and re-filling the flume during the tests, a common practice potentially disturbing the bed surface (Ockelford and Haynes, 2013), photographs of the bed after armoring with Q_1 were obtained through water (H = 0.13 m). The flow rate was reduced substantially to remove surface waves and to record clear images. The armors formed with Q_2 were photographed both through water and in air, at the end of each run. The maximum relative difference in terms of D_{50} was 1.4%, demonstrating the intrinsic robustness of the methodology.

High-resolution DEMs of the gravel-bed surface (area: 1 × 0.45 m^2, grid spacing: 1 mm, theoretical depth resolution: 0.35 mm) were reconstructed from three overlapping stereo photographs, using the technique presented in Bertin et al. (2015). Camera calibration was performed in-situ at the beginning of a test using a flat chequerboard, before the recess was loaded with sediment, to allow subsequent topography measurements both in air and through water. To measure through water, it was critical to keep the water depth constant (H = 0.13 m was used) for all image acquisition (Bertin et al., 2013). Using photogrammetry, depth is triangulated at each pixel location (pixel size ~0.15 mm), and shadowed points are interpolated based on the assumption of a continuous surface, leaving no voids in the point clouds. Point clouds were interpolated onto raster DEMs with 1 mm grid spacing. Relative DEM accuracy was estimated by comparing DEMs of the armors formed with Q_2 measured in air with those measured through water, resulting in MUE = 0.66 ± 0.11 mm, and SDE = 1.01 ± 0.10 mm (i.e. mean ± 1 standard deviation, n = 6). Before analysis, the DEMs were resized to 0.8 × 0.3 m^2 to minimize flume wall influence. Similar to previous research, DEMs were detrended to remove any surface trend that could bias the grain-roughness properties of interest (e.g., Aberle and Nikora, 2006; Hodge et al., 2009), such as linear trend surfaces representing the combined effect of flume-bed slope and setup misalignment (when the cameras are not perfectly parallel to the flume bed, causing a tilt in the DEM). Any low-amplitude bedform on the gravel-bed surface, larger than particle clusters,

was also removed in a second step, through the application of a moving filter of radius $1.25D_{90A}$ (Smart et al., 2002). DEMs were finally normalized to have a zero-mean bed elevation.

For all experimental runs, detrended DEMs were first analyzed in terms of standard deviation (σ_Z), range (Δ_Z) and skewness (S_K). The latter are bed-elevation moments contained in probability distribution functions (PDFs) and classical descriptors of bed roughness.

Generalized second-order structure functions of detrended bed elevations were also obtained:

$$D_{G2}(\Delta x, \Delta y) = \frac{1}{(N-n)(M-m)} \sum_{i=0}^{N-n} \sum_{j=0}^{M-m} \{|z(x_i + n\delta x, y_j + m\delta y) - z(x_i, y_j)|\}^2 \quad [1]$$

where, $\Delta x = n\delta x$ and $\Delta y = m\delta y$; δx and δy are the sampling intervals (both 1 mm) in the longitudinal and transverse directions respectively; n=1,2,3,…N and m=1,2,3,…M. N and M are the number of samples (801 and 301, respectively) in the same two directions. The maximum spatial lag in both x and y directions was chosen as ±100 mm, being larger than the maximum particle size and sufficient to reach the saturation region. Horizontal (grain-) roughness indices ΔX_0 and ΔY_0 were determined from 1D structure functions, in both x and y directions (Nikora et al., 1998). Because analyzed DEMs were detrended, observed patterns of statistical elevation correlation indicate characteristics of grain size, shape and 2D arrangement on the bed surface.

Furthermore, the inclination index (I) was evaluated. The inclination index measures grain imbrication, by analyzing the signs of elevation changes between successive pairs of detrended DEM points at different lags, in different directions (Millane et al., 2006):

$$I(d, \theta) = \frac{n_+(d, \theta) - n_-(d, \theta)}{N(d, \theta)} \quad [2]$$

where n_+ and n_- are the number of positive and negative slopes, respectively, and N is the total number of slopes, all functions of the separation or lag d between pairs of DEM points and the angle θ formed with the flow direction. A positive slope was defined as increasing elevations along the flow direction. Inclination indices were computed using d = 1 mm, which is the DEM grid spacing. Slopes, whose absolute value was below 0.01, were deemed not reliable, and were not counted in the numerator of Eqn. 2 (Millane et al., 2006). We focused the analysis on I(0°), the inclination index measuring grain imbrication in the flow direction.

To test the hypothesis that stable armors are replicable under identical flow and sediment conditions, we compared the variability between replicated runs with the spatial variability within DEMs (inner variability), in terms of the different DEM properties measured during the study. All detrended DEMs were divided in three parcels of size 266 × 300 mm^2 and each DEM subset was analyzed independently. The coefficient of variation (CV) was calculated for each DEM as the standard deviation of the DEM property divided by the mean, and reported as a percentage, using the three DEM subsets, providing there were only positive values. Each DEM of the same sediment and surface type (e.g., all three armors formed with sediment 1 at the discharge Q_1) was characterized by the same inner variability for the different DEM properties. Hence, the CVs were averaged using all nine DEM subsets of the same surface type and sediment. We thus (1) compared the variability between replicated runs using the same sediment mixture and the average spatial variability within these same DEMs; (2) concurrently, a MATLAB® routine ensured no significant difference on the mean (i.e. average) values determined using the three subsets of any replicated surface, using paired t-tests at a confidence level α = 0.01. The observation of a similar variability (1) together with no significant difference on the mean (2) would lead to the conclusion that replicated surfaces cannot be distinguished.

3 RESULTS

The decline in sediment transport rate with armoring time (Figure 2) was well described by a relationship of the form $q_s = c.t^n$ (with c and n constants), which is characteristic of static armoring (e.g., Proffitt, 1980; Marion et al., 2003). Distinct trends in transport reduction were observed depending on the flow discharge, while no difference was observed between the sediment mixtures. The transport reduction during armoring with Q_2 was slower: only 30% of the total bedload charge was removed during the first 20 hours, with erratic transport up to 100 hours of armoring time.

Figure 3 shows the changes in bed-surface composition after armoring. Armoring with Q_1 altered the bed surface substantially, with a consistent increase for all percentiles (i.e. D_{16}, D_{50} and D_{84}). Application of Q_2 only

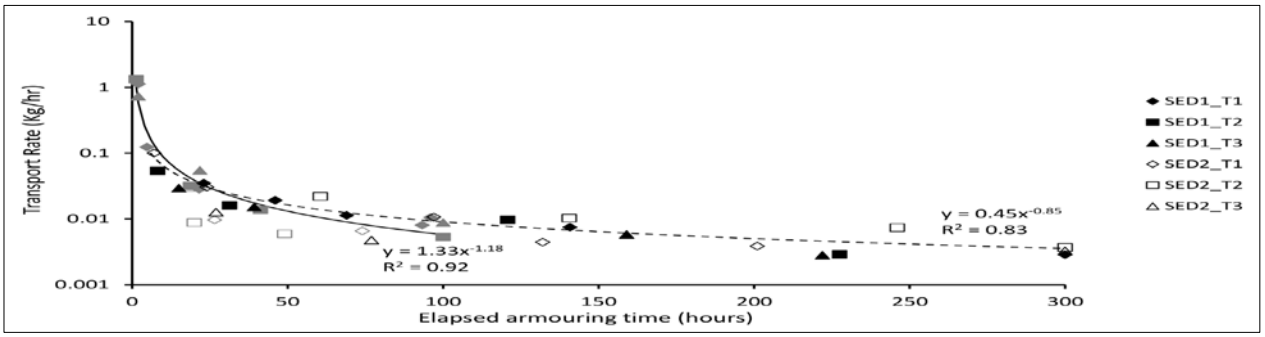

Figure 2. Sediment transport for all replicated runs during armoring with Q_1 on the initially screeded flat gravel-beds (grey markers and continuous line); and armoring with Q_2 on the beds previously armored with Q_1 (black markers and dashed line).

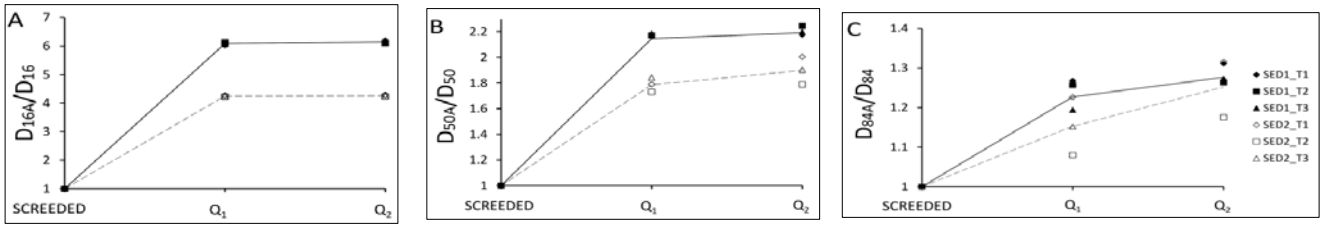

Figure 3. Bed surface composition, in terms of (A) D_{16}, (B) D_{50} and (C) D_{84}, for the different bed states (i.e. screeded, armored with Q_1 and armored with Q_2). Armor compositions obtained with Basegrain® (associated with the subscript "A") were normalized by the bulk mixture characteristics (Figure 1B). The lines represent the average trends for each sediment mixture (continuous black lines for sediment 1; dashed grey lines for sediment 2).

impacted the coarse end of the GSD. The greater variability in the armor D_{84} (i.e. D_{84A}), compared to D_{16A} and D_{50A}, likely relates to the preparation of the initial screeded beds and to the availability of coarse particles being uncovered by the flow. Measuring the armor ratio (defined as D_{50A}/D_{50}) shows that sediment 1 allowed the surface to armor more than the better-sorted sediment 2 (armor ratio of 2.2 and 1.8, respectively). The armor ratios were virtually unchanged despite re-armoring with Q_2 (paired t-test, no significant difference at $\alpha = 0.01$).

Preferential armor grains' orientation is presented in Figure 4. For both sediment mixtures, armor grains preferentially aligned their long axis (i.e. a-axis) with the flow direction during Q_1. The proportion of grains perpendicular to the flow was larger after Q_2 (Figure 4C).

Bed-elevation moments measured from the detrended DEMs are presented in Figure 5. The analysis reveals that the two sediment mixtures adjusted identically to the imposed flow rates in terms of distribution skewness, but evidences significant differences for the range and standard deviation (paired t-tests, $P < 0.05$).

Sediment 2 formed rougher surfaces for the two discharges, indicated by larger Δ_Z and σ_Z compared with sediment 1 (paired t-tests, $P < 0.05$). Only σ_Z changed significantly between Q_1 and Q_2 water-working (difference significant, $P < 0.05$), for both sediment mixtures, indicating surface roughening with discharge increases (e.g., Aberle and Nikora, 2006), whilst neither S_K nor Δ_Z values were significantly impacted.

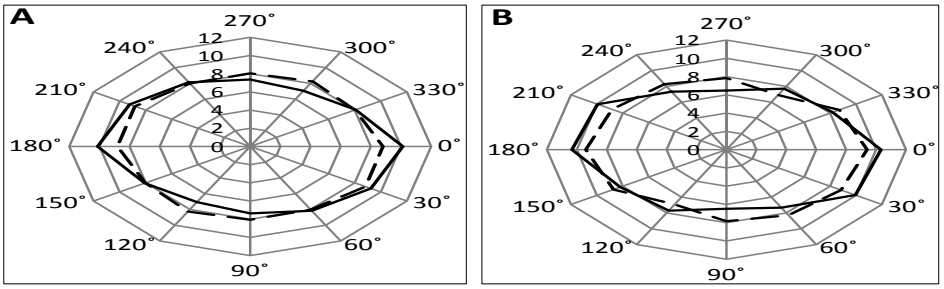

Figure 4. Frequency distribution of bed-surface material for different a-axis orientations, with (A) sediment 1 and (B) sediment 2. The general tendency for each discharge is presented (continuous line for Q_1; dashed line for Q_2), which was obtained by averaging the results over the three replicated runs.

Results obtained from second-order structure functions are presented in Figure 5D and 5E**.** It is shown that both sediment mixtures formed armors with identical horizontal grain-roughness indices (paired t-test, P <

0.01), in both the downstream and transverse directions. Grain-roughness indices in the flow direction were on average longer than cross-flow indices, and both indices increased with discharge (differences significant at α = 0.01).

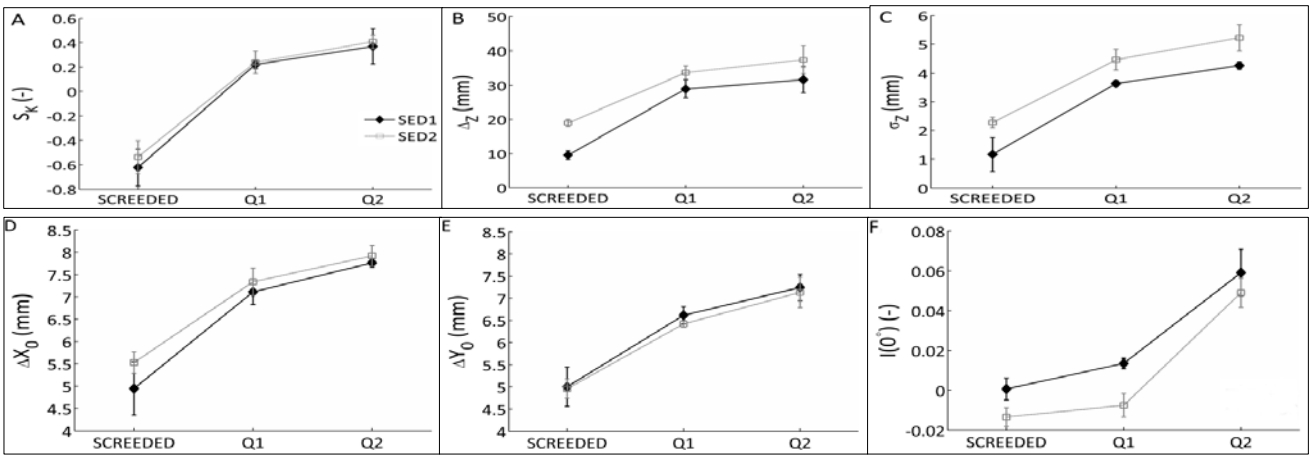

Figure 5. (A) skewness (S_K), (B) range (Δ_Z) and (C) standard deviation (σ_Z) of detrended bed elevations for all replicated runs. (D, E) are the horizontal grain-roughness indices (ΔX_0, ΔY_0) determined from 2nd-order structure functions along (D) the downstream (x), and (E) the transverse (y) direction. (F) is the inclination index representing grain imbrication in a direction parallel to the flow (θ = 0°). The trend for each sediment mixture is presented, which was obtained by averaging the results over the three replicated runs. The error bars have a length equal to two times the standard deviations, centered on the mean value.

Figure 5F shows results for the inclination index, measuring grain imbrication in the flow direction. Screeded beds were characterized by a negative or near zero (0°), suggesting no grain imbrication. Only the beds made of sediment 1 showed grain imbrication after armoring with Q_1. However, the small inclination index values (≃0.0175) suggest that imbrication was weak and limited to small portions of the bed. Q_2 was competent enough to imbricate particles for both sediment mixtures.

Table II compares the variability between replicated surfaces and the average (inner) variability within these same surfaces, for the parameters measured in this study, using the percent coefficient of variation (CV). It shows firstly that armored beds have smaller CVs, therefore are more consistent, both spatially and between replicated runs than screeded beds prepared manually. Secondly, the difference in variability between replicated armors and within DEMs is small, even suggesting a larger variability within DEMs than between replicated runs. In parallel, we verified the hypothesis that the mean (i.e. average) property values determined using the three subsets of any replicated run do not differ statistically using paired t-tests (α = 0.01), for the different DEM properties.

Table II: Variability (using the percent coefficient of variation, CV) between and within replicated surfaces. The variability within a DEM was measured using three DEM subsets of size 266 × 300 mm^2. N.A stands for non-applicable, because of the existence of negative values, preventing the use of the coefficient of variation.

			S_K	σ_Z	ΔX_0	ΔY_0	I(0°)
SEDIMENT 1	Averaged CV	Screeded	*N.A*	12.7	3.5	2.5	*N.A*
	within DEMs	After Q_1	47.1	6.1	4.0	3.1	70.6
		After Q_2	32.8	5.1	1.4	1.9	31.5
	CV between	Screeded	*N.A*	16.1	12.1	8.8	*N.A*
	repeat runs	After Q_1	15.5	2.6	4.0	2.9	19.7
		After Q_2	38.8	4.0	1.3	4.1	19.8
SEDIMENT 2	Averaged CV	Screeded	*N.A*	16.1	6.0	5.0	*N.A*
	within DEMs	After Q_1	87.6	5.2	2.6	4.1	*N.A*
		After Q_2	16.6	6.7	2.5	4.1	71.3
	CV between	Screeded	*N.A*	13.1	4.3	4.3	*N.A*
	repeat runs	After Q_1	38.8	12.3	4.2	1.1	*N.A*
		After Q_2	13.6	1.2	2.9	4.8	15.0

4 DISCUSSION

The use of a vertically adjustable test section in our tests allowed analysis of bed degradation under consistent bed shear stress, which was critical to study armor replicability. The progressive transport reduction characteristic of static armors (Proffitt, 1980; Marion et al., 2003) was consistent throughout the six runs (R^2 =

0.92 and 0.83 for Q_1 and Q_2, respectively), which verified that the sediment recess was correctly adjusted upwards for all runs according to the rate of bed degradation (Figure 2).

In accordance with previous works, which showed that armor composition is specific given the parent bed material and formative discharge during parallel degradation (e.g., Garde et al., 2006), our armor composition replicated well between runs using the same sediment, yet varied substantially between the two sediment mixtures (Figure 3). The latter can be explained by different flow competencies. Increasing the flow discharge from Q_1 to Q_2 did not alter the degree of armoring (unchanged armor ratio), suggesting the persistence of the armor formed with Q_1 and constant roughness effects.

In contrast, we measured changes in grain orientation during Q_2, with increasing grains aligned perpendicular to the flow direction (Figure 4). Furthermore, grain roughness increased during Q_2, as shown by increasing σ_Z values (Figure 5C). This strengthens the argument that fluvial surfaces react to moderate changes in flow strength through a variety of processes.

Likewise, we measured increases in horizontal roughness length with armoring (Figure 5D, 5E), which can be explained by surface coarsening (Figure 3) and particle grouping. Observations of grain imbrication also support surface alterations due to armoring (Figure 5F). Armors formed with Q_2 presented accentuated grain imbrication, compared to the armors formed with the lower discharge Q_1.

Hence, despite difficulties preparing the screeded beds identically at the beginning of each run, due to the random distribution of coarse particles near the surface after manual preparation of the beds, our experimental data showed that water-working had a notable effect for the initial random sediment organization, creating more pronounced patterns, such as grain packing and grouping, interlocking and imbrication. We observed an augmented surface consistency (Table II), together with a similar variability in armor properties between repeat armors and within these same surfaces. Together with our finding that mean values, measured using the three subsets of any replicated surface, were consistent, this provides strong evidence for armor replicability - for a given formative discharge and parent bed material. This finding has been assumed previously (e.g., Aberle and Nikora, 2006), yet never proven.

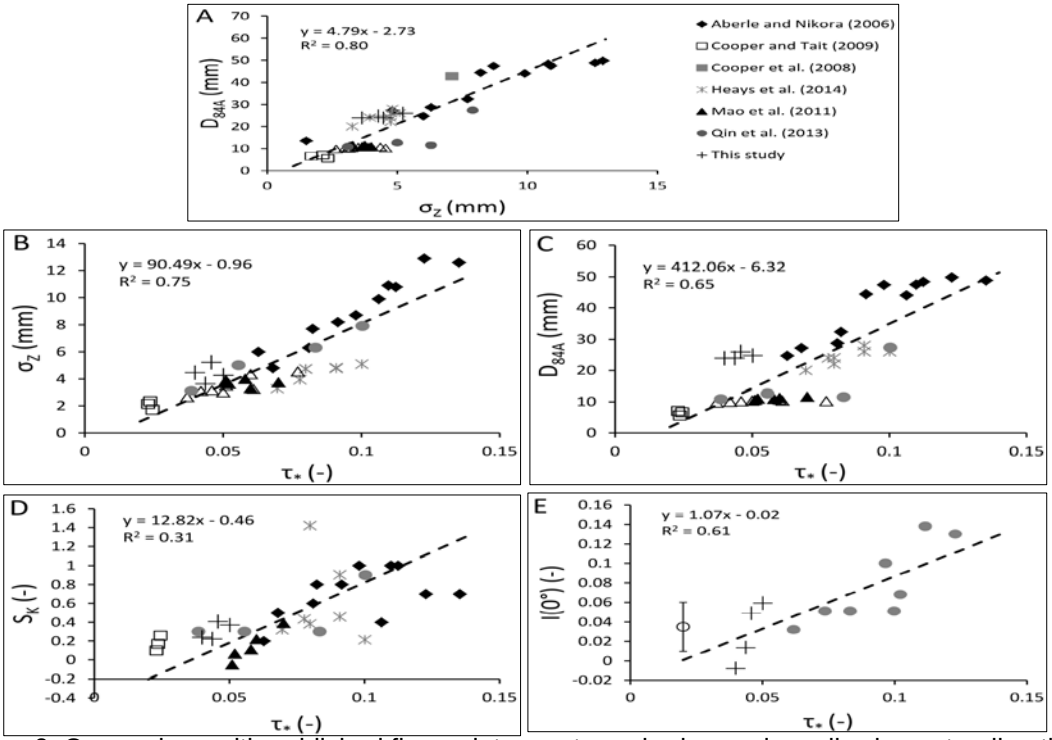

Figure 6. Comparison with published flume data on streambed armoring, allowing extending the analysis of the formative controls on gravel-bed armors. Open markers correspond to mobile armors (formed with either sediment feeding or sediment recirculating). The open round marker in subplot (E) corresponds to data from *Pledger et al.* (2014). In the case data was not collated in tables, it was digitized from graphs with the best care possible. Depending on the data source, the Shields stress had to be re-calculated from the shear stress and the bulk mixture D_{50}. Dashed lines are the functional lines best representing the data (Mark and Church, 1977).

When compared with previous studies on stable armor composition (e.g., Garde et al., 2006), our experimental results therefore suggest that a gravel-bed's response is specific to the formative parameters. To strengthen this argument and to provide a broader context for our findings, we combined our experimental results with those from previous flume studies on streambed armoring (Figure 6). The combined analysis of 43

gravel armors, of which 12 were mobile armors (Cooper and Tait, 2009; Mao et al., 2011; Pledger et al., 2014), extended the range of parent bed (D_{50} = [4 - 11] mm) and formative discharge (τ_* = [0.02 - 0.14]) and allowed extending the analysis of the effects of discharge and bed composition on the armor properties. The extended dataset presented in Figure 6A confirms the strong link between armor composition and armor topography. A better agreement was observed between D_{84A} and σ_Z, compared to D_{50A} and σ_Z (R^2 = 0.80 and R^2 = 0.62, respectively), suggesting that the arrangement of coarse grains on the surface, which protrude higher into the flow and form the anchor for small-scale bedforms (e.g., Piedra et al., 2012), is an essential control on gravel-bed topography. Because of the good relationship between armor σ_Z and grain-size properties, commonly researchers suggest the interchangeable use of σ_Z, D_{50A} and D_{84A} as indicators of surface roughness. However, we observed in this study that armor topography is more sensitive to changes in flow discharge than armor composition, and shows a better relationship with the Shields stress (Figures 6B and 7C). The analysis of 43 gravel armors showed that σ_Z, S_K and I(0°) increase with Shields stress, confirming previous assumptions of a strong control of flow discharge on armor topography (e.g., Aberle and Nikora, 2006; Mao et al., 2011). Figure 6E shows that streamwise particle imbrication increases with transport capacity, supporting past statements that imbrication forms as a result of the entrainment of the coarse sediment fraction in a mixture (Rust, 1972).

5 CONCLUSIONS

Experimental gravel beds, water-worked in a laboratory flume under conditions of zero sediment feed and selective transport, have been analyzed using a range of accepted statistical methods in order to examine the formative controls for gravel-bed armors. The use of photogrammetric techniques enabled a detailed characterization of gravel-bed surfaces and their adjustments to competent flows. We presented the efficient and effective measurement of bed composition and topography through water, which obviated the need to drain and refill the flume in-between measurements.

We showed that bed topography (structure) was more responsive to changes in flow discharge and displayed more degrees of adaptability than bed material size alone. Our experimental data supported the hypothesis that stable armor properties are replicable under identical flow and sediment conditions. This suggests that in conditions of parallel degradation, gravel-bed's response to water-work is specific to the formative parameters, even though the inherent mechanisms for the armor layer formation are stochastic. The addition of independent data from previous flume studies on streambed armoring illustrated the importance of two formative controls on armor structure: the Shields stress and the parent bed composition.

Future work may try to further our understanding of the effect of sediment supply and flow duration onto armor properties formed in the laboratory, which would ultimately allow more realistic investigations of field processes.

ACKNOWLEDGMENTS

The study was partly funded by the Marsden Fund (Grant No. UOA1412), administered by the Royal Society of New Zealand. The authors would like to thank M. Dequidt and S. Stähly for their assistance during the experimental programme.

REFERENCES

Aberle, J. & Nikora, V. (2006). Statistical Properties of Armored Gravel Bed Surfaces. *Water Resource Research,* 42(11), 1-11.

Bertin, S., Friedrich, H., Delmas, P. & Chan, E. (2013). On the use of Close-Range Digital Stereo-Photogrammetry to Measure Gravel-Bed Topography in a Laboratory Environment. *35th IAHR Congress,* Chengdu, China.

Bertin, S., Friedrich, H., Delmas, P., Chan, E. & Gimel'farb, G. (2015). Digital Stereo Photogrammetry for Grain-Scale Monitoring of Fluvial Surfaces: Error Evaluation and Workflow Optimisation. ISPRS *Journal of Photogramm and Remote Sensing,* 101, 193-208.

Chin, C., Melville, B. & Raudkivi, A. (1994). Streambed Armoring. *Journal of Hydraulic Engineering,* 120(8), 899-918.

Clayton, J.A. & Pitlick, J. (2008). Persistence of the Surface Texture of a Gravel-Bed River during a Large Flood. *Earth Surface Processes and Landforms,* 33(5), 661-673.

Cooper, J.R. & Tait, S.J. (2009). Water-Worked Gravel Beds in Laboratory Flumes - A Natural Analogue? *Earth Surface Processes and Landforms,* 34(3), 384-397.

Detert, M. & Weitbrecht, V. (2012). *Automatic Object Detection to Analyze the Geometry of Gravel Grains*. Riverflow 2012, San Jose, Costa Rica, Taylor And Francis Group.

Fehr, R. (1987). *Geschiebeanalysen in Gebirgsflüssen Translated Analysis of Sedimentary Bed Material in Mountain Rivers*, *Conversion and Comparison of Various Analytical Methods*. Mitteilungen Derversuchsanstalt Fürwasserbau, Hydrologie Und Glaziologie, Eidgenössische Technische Hochschule, Zürich, Nr. 92.

Garde, R.J., Sahay, A. & Bhatnagar, S. (2006). A Simple Mathematical Model to Predict the Particle Size Distribution of the Armour Layer. *Journal of Hydraulic Research,* 44(6), 815-821.

Gessler, J. (1967). *The Beginning of Bedload Movement of Mixtures Investigated as Natural Armoring in Channels. Pasadena, Calif*. W.M. Keck Laboratory of Hydraulics and Water Resources, California Institute of Technology.

Gomez, B. (1983). Temporal Variations in Bedload Transport Rates: The Effect of Progressive Bed Armouring. *Earth Surface Processes and Landforms,* 8(1), 41-54.

Gomez, B. (1993). Roughness of Stable, Armored Gravel Beds. *Water Resource Research,* 29(11), 3631-3642.

Gomez, B. (1994). Effects of Particle Shape and Mobility on Stable Armor Development. *Water Resource Research,* 30(7), 2229-2239.

Haschenburger, J.K. & Wilcock, P.R. (2003). Partial Transport in a Natural Gravel Bed Channel. *Water Resource Research,* 39(1), 1-9.

Heays, K.G., Friedrich, H. & Melville, B.W. (2014). Laboratory Study of Gravel-Bed Cluster Formation and Disintegration. *Water Resource Research,* 50(3), 2227-2241.

Hodge, R., Brasington, J. & Richards, K. (2009). Analysing Laser Scanned Digital Terrain Models of Gravel Bed Surfaces: Linking Morphology to Sediment Transport Processes and Hydraulics. *Sedimentology,* 56(7), 2024-2043.

Hodge, R.A., Sear, D.A. & Leyland, J. (2013). Spatial Variations in Surface Sediment Structure in Riffle–Pool Sequences: A Preliminary Test of the Differential Sediment Entrainment Hypothesis (DSEH). *Earth Surface Processes and Landforms,* 38(5), 449-465.

Lane, S.N. (2005). Roughness – Time For A Re-Evaluation? *Earth Surface Processes and Landforms,* 30(2), 251-253.

Laronne, J.B. & Carson, M.A. (1976). Interrelationships Between Bed Morphology and Bed-Material Transport For a Small, Gravel-Bed Channel. *Sedimentology,* 23(1), 67-85.

Mao, L., Cooper, J.R. & Frostick, L.E. (2011). Grain Size And Topographical Differences Between Static And Mobile Armour Layers. *Earth Surface Processes and Landforms,* 36(10), 1321-1334.

Marion, A., Tait, S.J. & Mcewan, I.K. (2003). Analysis of Small-Scale Gravel Bed Topography during Armoring. *Water Resource Research,* 39(12), 1-11.

Mark, D.M. & Church, M. (1977). On the Misuse of Regression In Earth Science. *Journal of the International Association for Mathematical Geology,* 9(1), 63-75.

Millane, R.P., Weir, M.I. & Smart, G.M. (2006). Automated Analysis of Imbrication and Flow Direction in Alluvial Sediments Using Laser-Scan Data. *Journal of Sedimentary Res*earch, 76(8), 1049-1055.

Nikora, V.I., Goring, D.G. & Biggs, B.J.F. (1998). On Gravel-Bed Roughness Characterization. *Water Resource Research,* 34(3), 517-527.

Ockelford, A.-M. & Haynes, H. (2013). The Impact of Stress History on Bed Structure. *ESPL,* 38(7), 717-727.

Odgaard, A.J. (1984). Grain Size Distribution of Riverbed Armor Layers. *Journal of Hydraulic Engineering,* 110(10), 1479-1484.

Paris, E. (1992). Time-Space Bed Load Evolution in Static Armour Formation. *Grain Sorting Seminar*, Ascona, Switzerland, Eidgenössische Technische Hochschule Zürich, Switzerland.

Parker, G. & Klingeman, P.C. (1982). On Why Gravel Bed Streams are Paved. *Water Resource Research.,* 18(5), 1409-1423.

Parker, G. & Sutherland, A.J. (1990). Fluvial Armor. *Journal of Hydraulic Research,* 28(5), 529-544.

Piedra, M.M., Haynes, H. & Hoey, T.B. (2012). The Spatial Distribution of Coarse Surface Grains and the Stability of Gravel River Beds. *Sedimentology,* 59(3), 1014-1029.

Pitlick, J., Mueller, E.R., Segura, C., Cress, R. & Torizzo, M. (2008). Relation Between Flow, Surface-Layer Armoring and Sediment Transport in Gravel-Bed Rivers. *Earth Surface Processes and Landforms,* 33(8), 1192-1209.

Pledger, A.G., Rice, S.P. & Millett, J. (2014). Reduced Bed Material Stability and Increased Bedload Transport Caused by Foraging Fish: A Flume Study with Juvenile Barbel (Barbus Barbus). *Earth Surface Processes and Landforms,* 39(11), 1500-1513.

Proffitt, G.T. (1980). Selective Transport and Armouring of Non-Uniform Alluvial Sediments, *PhD Thesis*. Department of Civil Engineering. Christchurch, University of Canterbury.

Richards, K. & Clifford, N. (1991). Fluvial Geomorphology: Structured Beds in Gravelly Rivers. *Progress In Physical Geography,* 15(4), 407-422.

Rust, B.R. (1972). Pebble Orientation in Fluvial Sediments. *Journal of Sedimentary Research,* 42(2), 384-388.

Smart, G., Duncan, M. & Walsh, J. (2002). Relatively Rough Flow Resistance Equations. *Journal of Hydraulic Engineering,* 128(6), 568-578.

Vericat, D., Batalla, R.J. & Garcia, C. (2006). Breakup and Reestablishment of the Armour Layer in a Large Gravel-Bed River Below Dams: The Lower Ebro. *Geomorphology,* 76(1–2), 122-136.

Wilcock, P.R. & Detemple, B.T. (2005). Persistence of Armor Layers in Gravel-Bed Streams. *Geophysical Research Letter,* 32(8).

